

## Supporting Information

### When photoluminescence, electroluminescence, and open-circuit voltage diverge – perovskite solar cells with and without phase segregation

Firouzeh Ebadi<sup>1,2</sup>, Bowen Yang<sup>1</sup>, Yeonju Kim<sup>1</sup>, Raheleh Mohammadpour<sup>2</sup>, Nima Taghavinia<sup>2,3</sup>, Anders Hagfeldt<sup>1</sup>, Wolfgang Tress,<sup>1,4\*</sup>

<sup>1</sup>École Polytechnique Fédérale de Lausanne, Laboratory of Photomolecular Science, 1015 Lausanne, Switzerland.

<sup>2</sup>Institute for Nanoscience and Nanotechnology, Sharif University of Technology, Tehran 14588, Iran.

<sup>3</sup>Department of Physics, Sharif University of Technology, Tehran 14588, Iran.

<sup>4</sup>Institute of Computational Physics, Zurich University of Applied Sciences, Wildbachstr. 21, 8401 Winterthur, Switzerland

**Table SI1.** Solar cell parameters measured under solar simulator.

Perovskite	J <sub>sc</sub> (mA/cm <sup>2</sup> )	V <sub>oc</sub> (V)	FF	PCE %
Cs <sub>0.1</sub> FA <sub>0.9</sub> PbI <sub>3</sub>	22.18 ± 0.51	0.953 ± 0.027	0.68 ± 0.04	15.24 ± 1.39
Cs <sub>0.1</sub> FA <sub>0.9</sub> Pb(I <sub>0.65</sub> Br <sub>0.35</sub> ) <sub>3</sub>	17.18 ± 0.66	1.137 ± 0.020	0.66 ± 0.02	13.52 ± 1.06

**Table SI2.** Fitting parameters for the EL data shown in Fig. 5

Time (s)	σ <sub>1</sub> (nm)	σ <sub>2</sub> (nm)	A <sub>1</sub>	A <sub>2</sub>	λ <sub>1</sub> (nm)	λ <sub>2</sub> (nm)
1250	40	51	1080	2942	729	776
1270	41	49	1413	3027	728.7	776
2760	43	48	1246	3437	737.5	782
2790	41	48	991	3588	733	781
4864	41	45	2648	3883	743	787
4884	41	46	1488	4049	738.9	785
4985	43	46	1135	3438	738	786
5004	45	45	952	3057	738.5	787
7930	41	45	6948	5206	746.4	789.6
7950	43	44	3544	4436	744	790
7970	43	44	2134	3728	742.4	789.5

7990	42	45	1584	3481	740.6	789
------	----	----	------	------	-------	-----

**Table SI3.** EQE EL of MAPb-halide compositions, determined at injection currents close to the respective short circuit current.

Composition	I:Br 1:1	I:Br 1:1	I:Br 1:2	Br	Br
EQE EL	6E-08	7E-07	1E-08	2E-08	5E-08

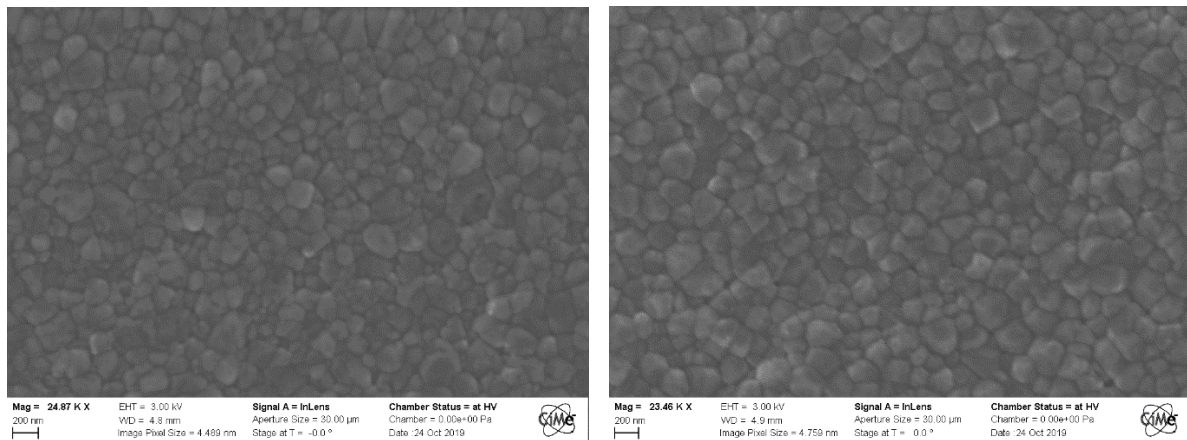


**Figure SI1.** SEM images of perovskite films with the two investigated compositions: (left)  $\text{Cs}_{0.1}\text{FA}_{0.9}\text{Pb}(\text{I}_{0.65}\text{Br}_{0.35})_3$ ; (right)  $\text{Cs}_{0.1}\text{FA}_{0.9}\text{PbI}_3$ . The morphology looks comparable.

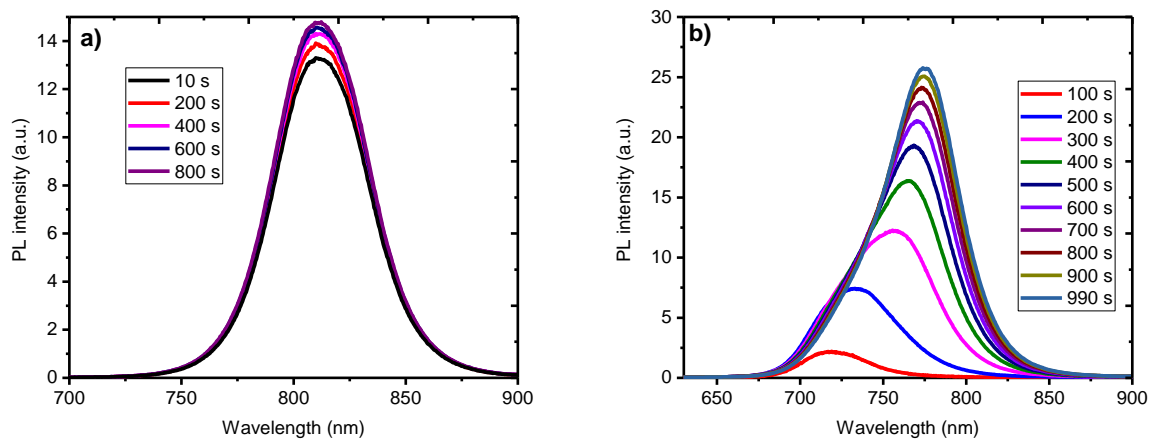


**Figure SI2.** PL spectra of (a) single halide and (b) mixed halide *films*.

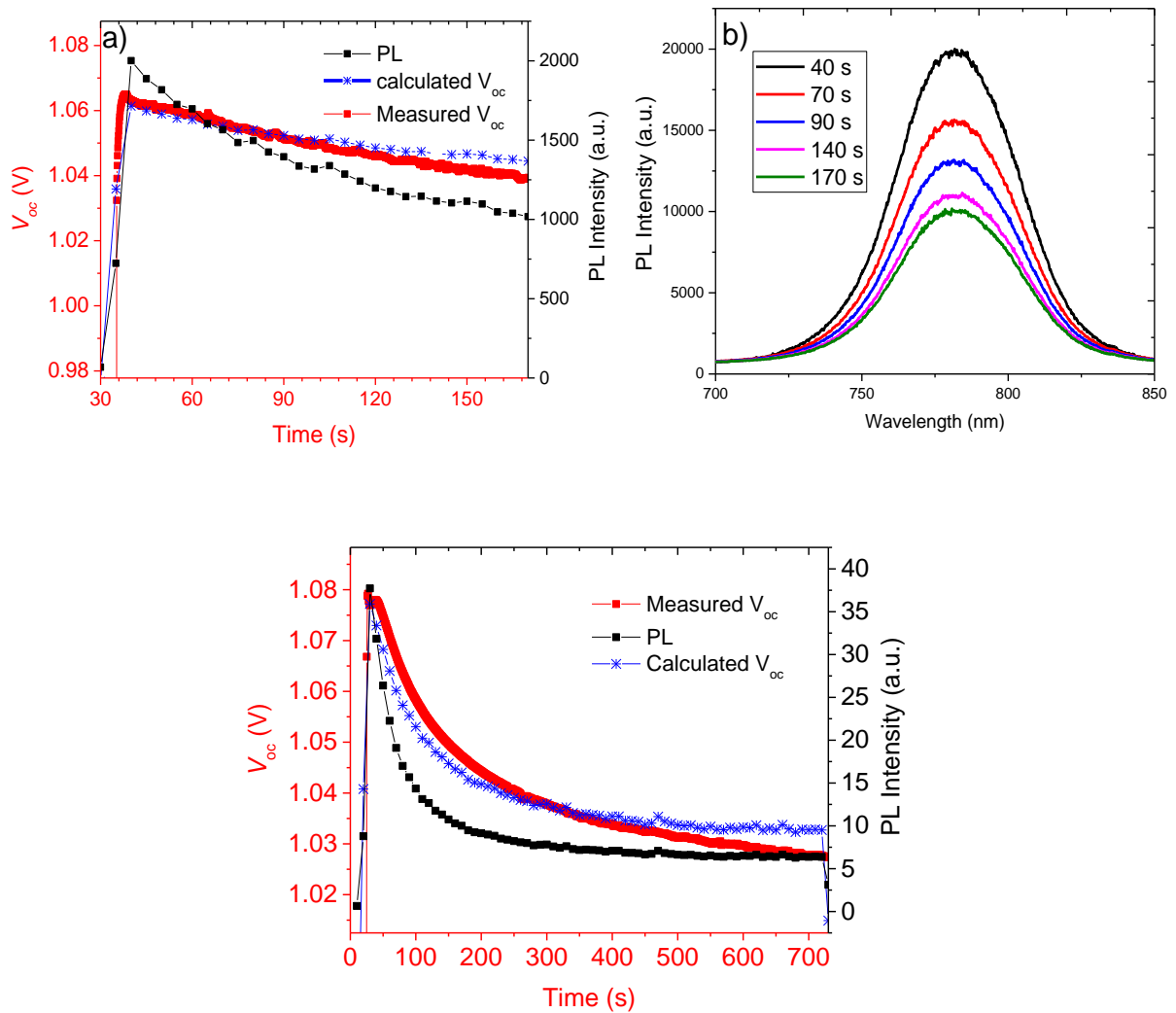


**Figure S13.** Examples of further compositions:  $\text{MAPbI}_3$  devices. (a) Evolution of PL,  $V_{oc}$  and calculated  $V_{oc}$  normalized at half of the time shown. (b) Corresponding PL spectra, whose shape remains but the intensity decreases. (c) A second sample, reproducing most of the trend. However, the slow but continuous decrease of  $V_{oc}$  at longer times is not well reproduced, possibly due to a low PL at  $V_{oc}$  compared to  $J_{sc}$  or enhanced gradients in the quasi-Fermi levels.

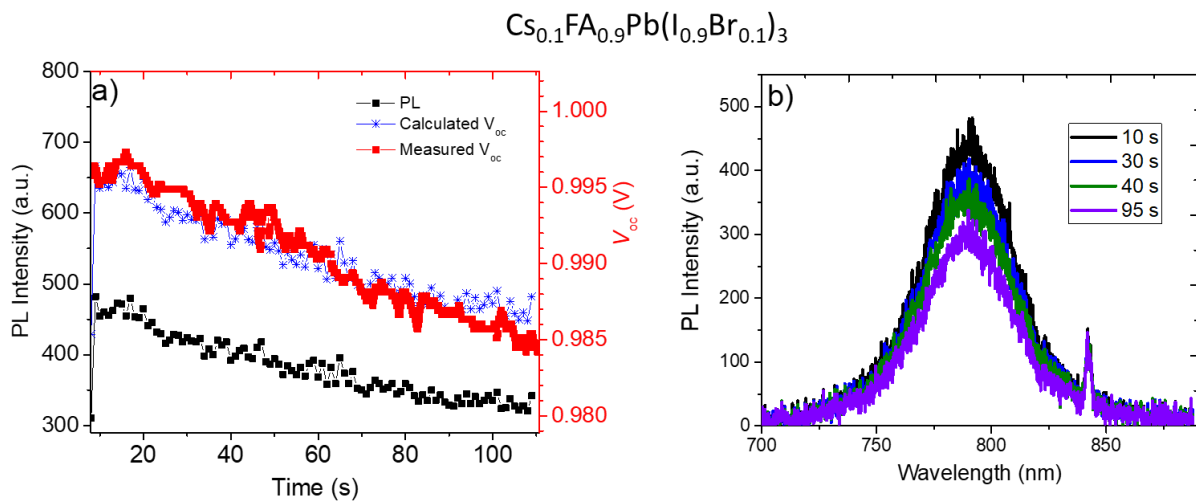


**Figure SI4.** Examples of further compositions:  $\text{Cs}_{0.1}\text{FA}_{0.9}\text{Pb}(\text{I}_{0.9}\text{Br}_{0.1})_3$  device. (a) Evolution of PL,  $V_{oc}$  and calculated  $V_{oc}$  normalized at half of the time shown. (b) Corresponding PL spectra, whose shape remains but the intensity decreases.

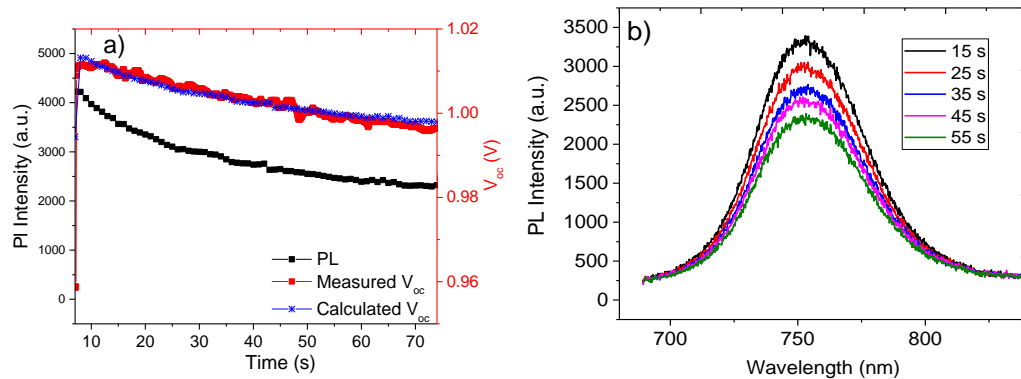


**Figure SI5.** Examples of further compositions:  $\text{MAPb}(\text{I}_{0.9}\text{Br}_{0.1})_3$  device. (a) Evolution of PL,  $V_{oc}$  and calculated  $V_{oc}$  normalized at half of the time shown. (b) Corresponding PL spectra, whose shape remains but the intensity decreases. The light intensity was ca. 3 W/cm<sup>2</sup>.

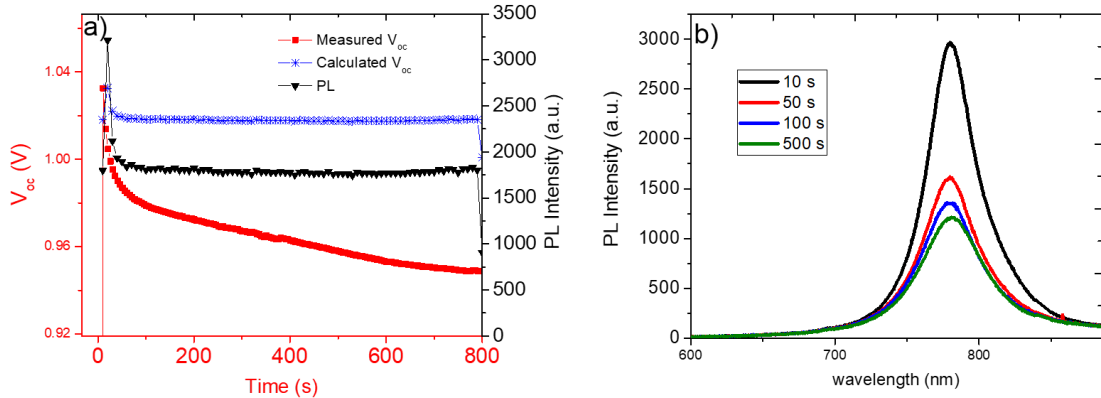
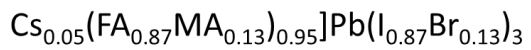


**Figure SI6.** Examples of further compositions: Triple cation device with instable  $V_{oc}$ . (a) Evolution of PL,  $V_{oc}$  and calculated  $V_{oc}$  normalized at half of the time shown. (b) Corresponding PL spectra, whose shape remains but the intensity decreases. In this case the decrease of  $V_{oc}$  at longer times is not well reproduced, possibly due to enhanced gradients in the quasi-Fermi levels.

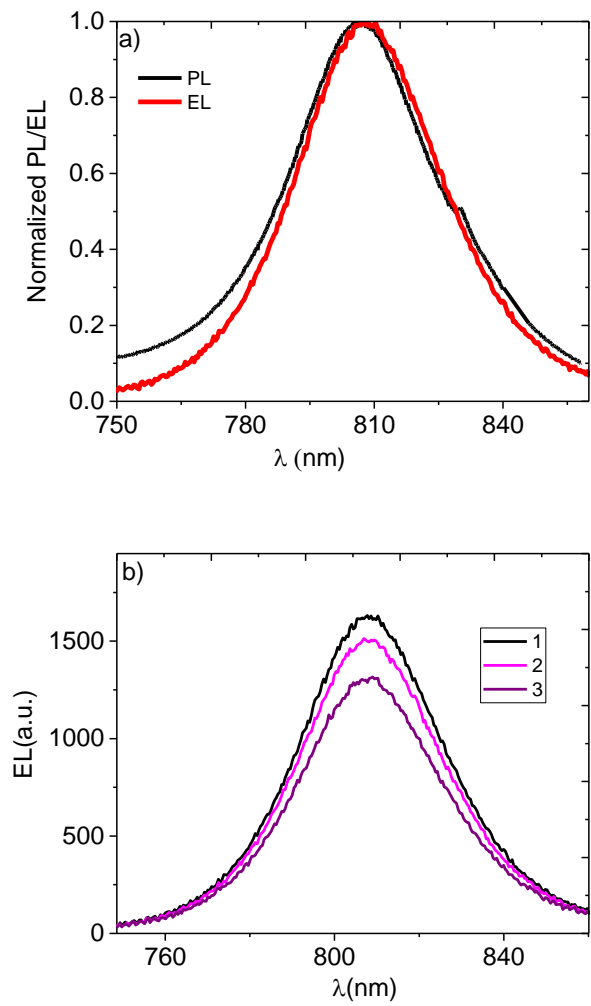


**Figure SI7.** Single-halide device. (a) Comparison of PL and EL spectra (b) Unchanged spectral shape but decreasing EL intensity during application of a constant current of 1 mA ( $3.6 \text{ mA}/\text{cm}^2$ )

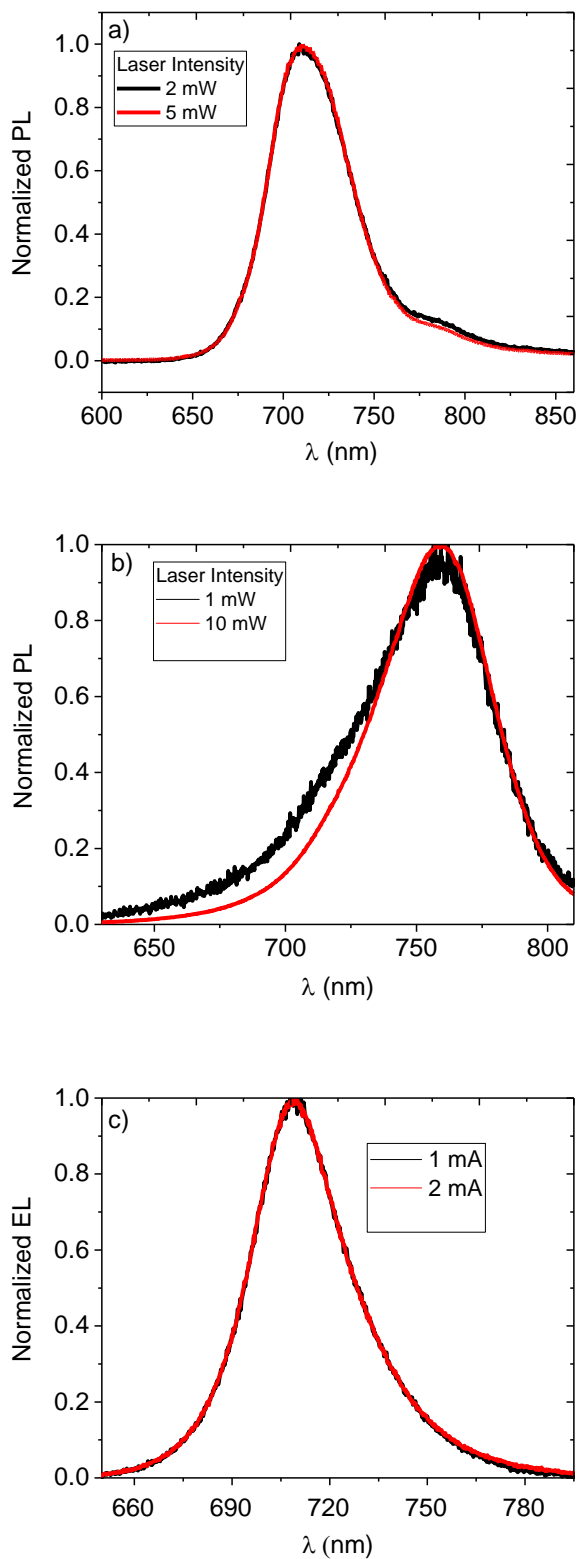


**Figure S18.** Mixed-halide device. (a) Normalized PL as a function of excitation intensity before light-soaking and (b) after light-soaking. (c) Normalized EL as a function of driving current.

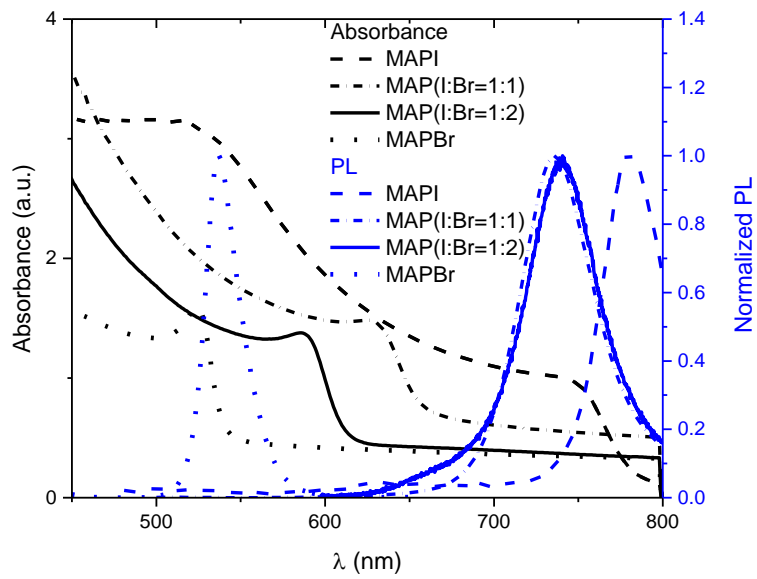
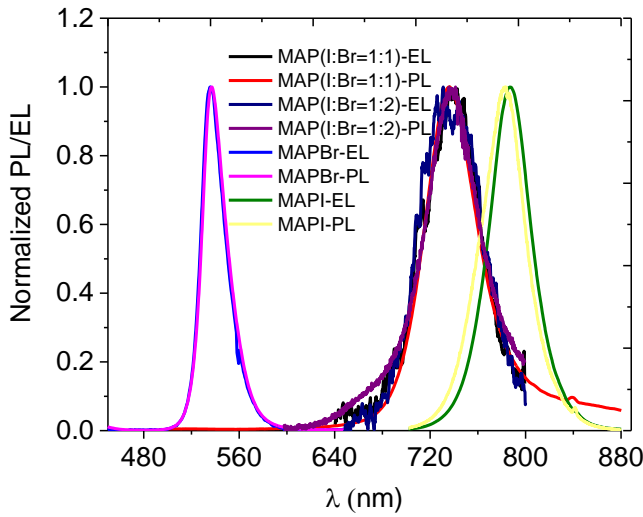
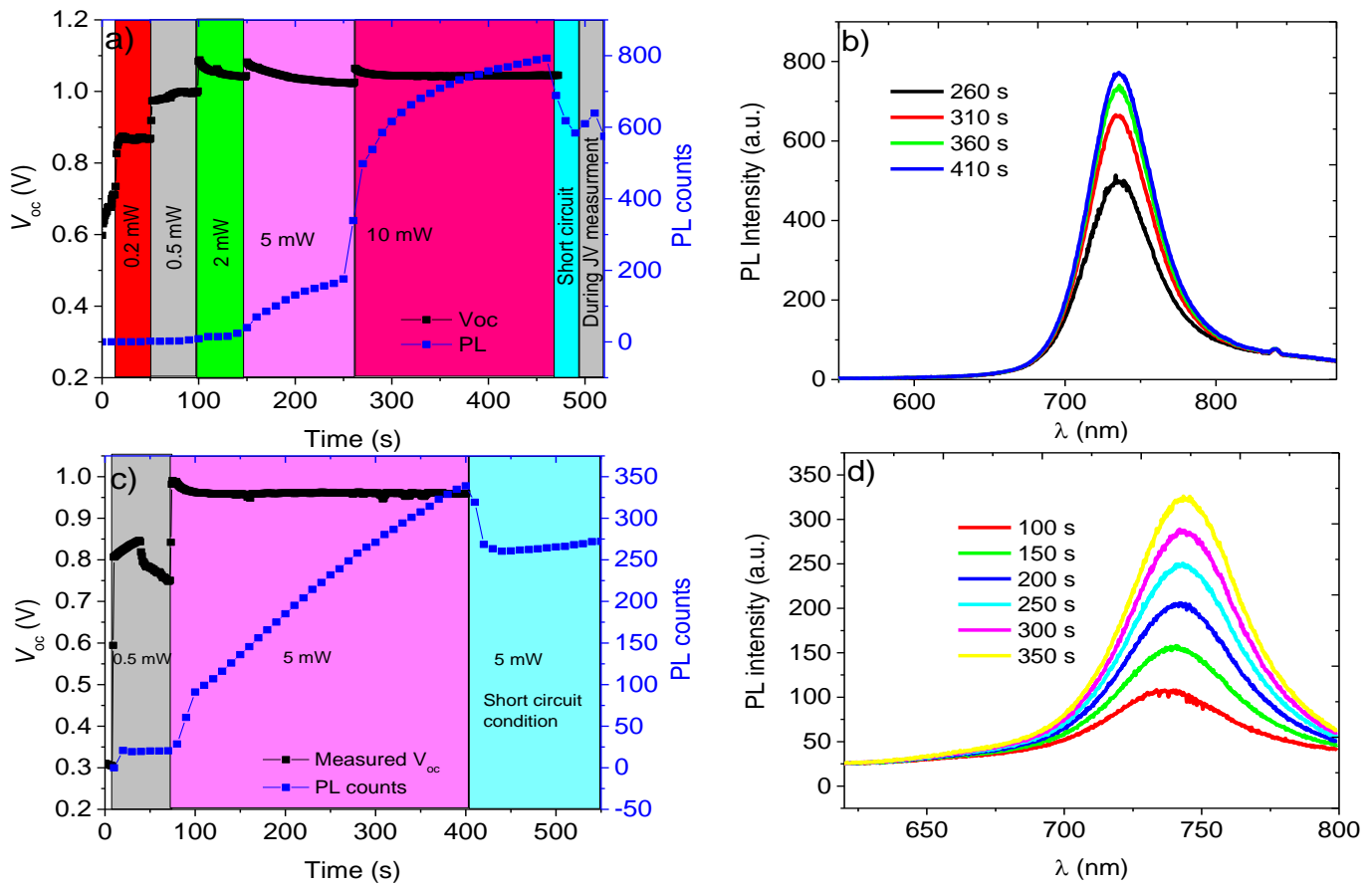


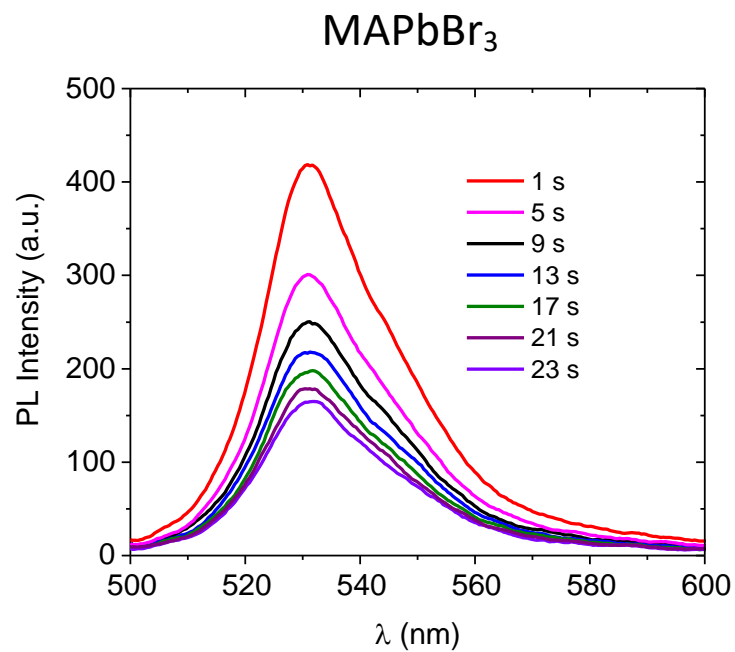
**Figure SI9.**  $\text{MAPb}(\text{I}_x\text{Br}_{1-x})_3$  series. Absorbance and PL of films for four compositions. The absorbance data contains also the scattered light, which is strongest for our 1:1 film. The mixed halide films show weak PL. Higher excitation densities lead to fast occurrence of the low-gap signal that is shown here. In our devices with the higher Br contents we could not study the evolution of light-induced halide segregation in detail as it was not reversible.



**Figures SI10.**  $\text{MAPb}(\text{I}_x\text{Br}_{1-x})_3$  series. Comparison of EL and PL for the four different Br concentrations. EL and PL are identical.



**Figures S11.**  $MAPb(I_xBr_{1-x})_3$  series. Evolution of  $V_{oc}$  and PL during light-soaking for the mixed halide film and corresponding PL spectra. (a), (b)  $I:Br = 1:1$ , (c),(d)  $I:Br = 1:2$ . The illuminated area was below approx.  $1\text{ mm}^2$ . Already after a first JV measurement, the low-gap phase is strongly pronounced and does not disappear completely in the dark. Therefore, spectra hardly shift but the PL intensity increases with different dynamics and opposite trend than the  $V_{oc}$ . This is qualitatively the same behavior as in the composition studied in detail in the main text.



**Figures SI12.** MAPb(I<sub>x</sub>Br<sub>1-x</sub>)<sub>3</sub> series. PL during light-soaking for MAPbBr<sub>3</sub> film. Light intensity was approx. 1 W/cm<sup>2</sup>.